Published in final edited form as:
Biomaterials. 2015 February ; 40: 61–71. doi:10.1016/j.biomaterials.2014.11.011.

Mesenchymal Stromal Cells form Vascular Tubes when Placed in Fibrin Sealant and Accelerate Wound Healing *in Vivo*

Julio J. Mendez[1], **Mahboobe Ghaedi**[1], **Amogh Sivarapatna**[1], **Sashka Dimitrievska**[1], **Zhen Shao**[2], **Chinedum Osuji**[2], **Derek M. Steinbacher**[3], **David J. Leffell**[4], and **Laura E. Niklason**[1,*]

[1]Departments of Anesthesiology and Biomedical Engineering, Yale University, New Haven, CT 06520

[2]Department of Chemical and Environmental Engineering, Yale University, New Haven, CT, USA

[3]Department of Surgery, Yale University School of Medicine, New Haven, CT, USA

[4]Department of Dermatology, Yale University School of Medicine, New Haven, CT, USA

Abstract

Non-healing, chronic wounds are a growing public health problem and may stem from insufficient angiogenesis in affected sites. Here, we have developed a fibrin formulation that allows adipose-derived mesenchymal stromal cells (ADSCs) to form tubular structures in vitro. The tubular structures express markers of endothelium, including CD31 and VE-Cadherin, as well as the pericyte marker NG2. The ability for the MSCs to form tubular structures within the fibrin gels was directly dependent on the stoichiometric ratios of thrombin and fibrinogen and the resulting gel concentration, as well as on the presence of bFGF. Fibrin gel formulations that varied in stiffness were tested. ADSCs that are embedded in a stiff fibrin formulation express VE-cadherin and CD31 as shown by PCR, FACS and immunostaining. Confocal imaging analysis demonstrated that tubular structures formed, containing visible lumens, in the stiff fibrin gels *in vitro*. There was also a difference in the amounts of bFGF secreted by ADSCs grown in the stiffer gels as compared to softer gels. Additionally, hAT-MSCs gave rise to perfusable vessels that were VE-cadherin positive after subcutaneous injection into mice, whereas the softer fibrin formulation containing ADSCs did not. The application of ADSCs delivered in the stiff fibrin gels allowed for the wounds to heal more quickly, as assessed by wound size, amount of granulation tissue and collagen content. Interestingly, following 5 days of healing, the ADSCs remained within the fibrin

*Corresponding author, Laura E. Niklason, 10 Amistad St., New Haven, CT 06519, Telephone: 203.737.1428, Fax: 203.737.1484, laura.niklason@yale.edu.

Author Contributions

L.E.N and J.J.M conceptualized and wrote the manuscript. J.J.M isolated MSCs, prepared fibrin gels performed FACS, immunostaining, and ELISA. M.G performed PCR on MSCs. A.S. performed subcutaneous injection/functional studies. S.D. performed rheological measurements. D.S. and D.L. conceptualized experiments.

Conflict of Interest:

L.E.N. has a financial interest in Humacyte, Inc, a regenerative medicine company. Humacyte did not fund these studies, and Humacyte did not affect the design, interpretation, or reporting of any of the experiments herein.

gel and did not integrate into the granulation tissue of healing wounds *in vivo*. These data show that ADSCs are able to form tubular structures within fibrin gels, and may also contribute to faster wound healing, as compared with no treatment or to wounds treated with fibrin gels devoid of ADSCs.

1. Introduction

Chronic wounds, and hard to heal wounds, are a common occurrence associated with vascular disease, injury, as well as irradiation following cancer treatment [1, 2]. Studies of cell-based therapy for the treatment of chronic wounds have largely centered on the use of ADSCs (MSCs) delivered topically, via a collagen or fibrin matrix, or directly injected into the edges of the wound [3–8]. The delivery of ADSCs using a fibrin spray to rodent wound models and in human clinical trials of non-healing wounds has demonstrated that MSCs can safely and effectively accelerate wound healing [3], which may occur through the secretion of growth factors or through a direct, cellular contribution to the healing wound [9]. ADSCs are particularly of interest since the isolation and propagation of patient-specific ADSCs is a relatively simple process, allowing for the *in vitro* expansion and banking these cells for future patient use. Additionally, the use of ADSCs in a clinical setting is currently an investigational cell therapy treatment for several diseases. This is largely because of the low clinical risk associated with the use of ADSCs [10].

ADSCs have been shown to play a supportive role in a transplantation setting [11] and in the formation of vascular tubes by endothelial cells *in vitro*, rather than by a direct contribution to vascular tube formation in the absence of endothelial cells [7, 12]. Recent studies using stem cells from the placenta demonstrated that placental stromal cells are capable of vascular tube formation in Matrigel in the absence of endothelial cells [13]. These stem cells from the placenta were positive for markers associated with ADSCs as well as other pluripotency markers, including: Oct-4, Klf-4 and Sox2, which are markers that are not typically associated with adult ADSCs [14]. Several recent papers have also described the ability of MSCs from various sources, including bone marrow [15], term amniotic membrane [16] , amniotic fluid [17], umbilical cord blood [18] and Wharton’s jelly [19] to differentiate into endothelial-like, tubular structures *in vitro*.

Furthermore, several papers have described the microenvironmental factors, including physical forces and soluble factors, which drive MSC differentiation toward an endothelial-like phenotype. Namely, these studies looked at shear force stimuli with exogenously added growth factors such vascular endothelial growth factor (VEGF) [20, 21], through genetic modification of MSCs to overexpress molecules such as VEGF [22] and pro-angiogenic molecule ephrin-B2 [23] or through addition of specific inhibitors, including simvastatin [24]. Additionally, groups have looked at the mechanical properties of the matrices that drive MSC differentiation, including culturing BM-MSCs on fibrin for osteoblastic differentiation [25], in polyethylene glycol dimethacrylate (PEGdma) gels [26] and in PEGylated fibrin gels [27].

Despite these prior studies, a detailed evaluation of ADSC behavior in fibrin gels alone, comparing different formulations of the gel delivery system, has not been addressed. We

hypothesized that ADSCs embedded within stiff, high-concentration fibrin gels could form more effective tubular structures *in vitro*. Therefore, in this study, we assessed the behavior of human adipose-derived mesenchymal stromal cells (ADSCs) in a human fibrin gel having a structural modulus of 3,000 Pa, as well as ADSC behavior within a softer fibrin gel, having a structural modulus of 1,650 Pa. Moreover, we implanted the ADSCs in fibrin gels subcutaneously in mice to assess the ability of the ADSCs to form tubular structures *in vivo*, and examined the expression of markers associated with endothelial cells, including CD31, VE-cadherin, as well as the pericyte marker NG-2. Finally, we sought to address whether the delivery of the ADSCs within the different composition fibrin gels resulted in an enhanced wound healing response compared with no treatment, or compared to delivery of fibrin gel devoid of cells. Overall, we highlight the importance of the composition of the fibrin mixture in driving the behavior of MSCs both *in vitro* and *in vivo*, as well as the contribution that ADSCs may have in the wound healing process.

2. Materials and Methods

2.1 Isolation, propagation and characterization of human adipose MSCs

A total of three adipose donors were used for these experiments, one male and two females; the age ranges of these donors were 44–63 years old. The human adipose tissue samples were isolated from anonymized and discarded tissue samples, and did not require Institutional Review Board (IRB) approval. Approximately 2 cc of discarded, anonymized human adipose tissue samples from liposuction surgery were harvested, washed with phosphate-buffered saline (PBS) and digested using collagenase type 1 (33 units/ml; Gibco, Grand Island, NY, USA, CAT # 17100-017) in high glucose Dulbecco's Modified Eagle's Medium (DMEM) in a final volume of 15 mL at 37°C for 60 minutes in a shaking incubator. The digest mixture was further mixed every 15 minutes of the 60 minutes incubation period by aspiration of the mixture through a 5 mL serological pipet. The digest was terminated by addition of 10% fetal bovine serum (FBS)/DMEM, followed by centrifugation of the sample at 1250 revolutions per minute (RPM) for 5 minutes. The supernatant containing mature adipocytes was discarded and the stromal cell fraction-containing pellet was re-suspended in medium containing 10% FBS/DMEM (high glucose). The yield of stromal cells from an initial 2 mL sample ranged from $0.3 \times 10^6 – 0.5 \times 10^6$ cells. These cells were plated at a concentration of 4,000–6,500 cells per cm^2. The cells were fed with medium, 10% FBS/DMEM (high glucose), every 2–3 days and passaged after 6–7 days when the cells were approximately 80% confluent.

All FACS antibodies were acquired from eBiosciences. The adhered cells were screened for markers at passages 2 and 5: CD90-FITC (11-0909-41), CD105-APC (17-1057-41), CD73-PE (12-0739-41), hematopoietic markers CD45-PE (12-9459-41), and mac1-APC (50-0112-80), as well as endothelial markers CD31-PE (PECAM-1, 12-0319-41) and CD144-PE (VE-cadherin, 12-1449-82). Species-specific isotype control antibodies used included: anti-mouse IgG-PE (12-4714), anti-mouse-FITC (11-4724) and anti-mouse IgG-APC (17-4015-80). For these analyses, adherent cells were washed 2 times with PBS, followed by incubation with 0.25% trypsin (Gibco) for 3 minutes. The cells were pelleted, washed in PBS and fixed in 2% PFA on ice for 10 minutes. The cells were then washed and

processed for FACS staining. Briefly, fixed cells were stained at the manufacturer's recommended dilution for 25 minutes on ice, followed by 2 washes in PBS. The cells were re-suspended in PBS and analyzed on a BD-LSRII FACS analyzer.

2.2 ADSC Culture in Fibrin Gels

Fibrin gel kits (Tisseel, Baxter, Deerfield, Ill) were used to re-suspend the ADSCs for *in vitro* culture. In both compositions, the ADSCs were re-suspended in the fibrinogen component of the Tisseel fibrin gel kit. The formulation of the fibrin gels is shown in Table 1 (Figure 2A). 2.5–3 × 10^6 ADSCs between passages 2–5 were re-suspended in medium (10% FBS/DMEM/1% P/S) and placed into the fibrinogen-containing syringe provided in the Tisseel Baxter fibrin kit. The other syringe contained the thrombin component. Approximately 250 μl was ejected through the tip of the dual-barrel syringe into 4-well chamber slides. Therefore, each chamber of the chamber slides contained on average 0.31 – 0.38 × 10^6 cells. The gel was allowed to fully polymerize for 5 minutes before applying culture medium (10% FBS/DMEM/1% P/S). The gel-containing cells were fed every 2–3 days for 7, 14 and 21 days prior to analysis.

2.3 Production of lentiviral vectors and ADSC lentiviral infection

Viral particles were produced and used to infect ADSC. Briefly, the lentiviral vector was generated by lipofectamin-mediated transfection of HEK 293T cells. Five million (5 × 10^6) 293T cells were cultured in 10 mL of DMEM/10% FBS medium in 10 cm^2 plates (Nunc) and transfected the following day with 10 g of transfer vector plasmid carrying the green fluorescent protein (*GFP)* gene, 2.5 μg of the pMD2G plasmid and 7.5 μg of the psPAX2 plasmid. Medium was removed at approximately 14–16 h post-transfection and replaced with 10 mL of fresh, preheated virus collecting medium. Supernatants were collected on post-transfection days 2 and 3 and filtered through a 0.4 μm pore size filter and concentrated 10-fold using an Amicon ultra centrifugal filter device (Millipore, Billerica, MA). The titer of the concentrated vectors was checked with HEK 293T cells. Then, ADSCs (1 × 10^5) at passage 2 or 3 were infected for 16 h with the GFP lentiviruses at MOI 30 in the presence of 4 μg/mL polybrene.

2.3 Rheological Measurements

The dynamic viscoelasticity of fibrin gels prepared with various concentrations of fibrinogen and thrombin was studied at 25°C using a rheometer with cone-plate geometry (MCR 301, Anton Paar). Samples were prepared by quickly transferring 1000 μL of each component from a double-barrel syringe directly to the plate of the 50 mm diameter, 2-degree cone-plate cell and mixed in place. To measure the gelation kinetics, the dynamic moduli of samples were monitored as a function of time using a fixed frequency of 1 rad/s and strain of 1%. Data were collected every 9 seconds for 1 hour.

2.4 qRT-PCR Analysis of ADSCs

The RNeasy Mini Kit from Qiagen was used to extract total RNA following the manufacturer's instructions. cDNA was synthesized with random hexamers as primers, using the SuperScript First-Strand Synthesis System according to manufacturer's protocol

(Invitrogen). An equal volume mixture of the products was used as templates for PCR amplification. All reactions were performed in 25 μl volume with iQ™ SYBR Green Supermix (Bio-Rad, Hercules, NY) and 200 nM each of forward and reverse primers shown using iCyler and iQ software (Bio-Rad). Samples were run in triplicate. PCR conditions included an initial denaturation step of 4 min at 95°C, followed by 40 cycles of PCR consisting of 15 s at 95°C, 30 s at 60°C, and 30 s at 72°C. Average threshold cycle (Ct) values from the triplicate PCR reactions for a gene of interest (GOI) were normalized against the average Ct values for GAPDH from the same cDNA sample. Fold change of GOI transcript levels between sample A and sample B equals $2^{-\Delta\Delta Ct}$, where $\Delta Ct = Ct_{(GOI)} - Ct_{(GAPDH)}$, and $\Delta\Delta Ct = \Delta Ct_{(A)} - \Delta Ct_{(B)}$. The expression of CD31, CD144 and GAPDH genes were identified by qPCR using the following primers:

CD31 forward: TGC AGT GGT TAT CAT CGG AGT G;

CD31 reverse: CGT TGT TGG AGT TCA GAA GTG;

CD144 forward: TCA CCT GGT CGC CAA TCC;

CD144 reverse: AGG CCA CAT CTT GGG TTC CT;

GAPDH forward: GACAACAGCCTCAAGATCATCAG;

GAPDH reverse: ATGGCATGGACTGTGGTCATGAG

2.5 Immunofluorescence Analysis and ELISA of ADSCs in Fibrin Gels

Fibrin gels containing ADSCs were fixed at days 7, 14, and 21 with cold 4% paraformaldehyde for 20 minutes. The gels were washed with PBS and processed for immunostaining as follows: 45 minutes incubation in blocking solution (10% normal goat serum/0.2% triton-X 100 in PBS), 2 hours in primary antibodies diluted in blocking solution, followed by 45 minutes of secondary antibodies diluted in blocking solution. All incubations were performed at room temperature in the dark. Primary antibodies used included: VE-cadherin 1/250 (Abcam), NG-2 1/50 (eBiosciences), and CD31 1/100 (Abcam). All secondary antibodies were purchased from the Alexa-Fluor antibody series from Invitrogen.

ELISA kits were purchased for human basic fibroblast growth factor (bFGF). The manufacturer's protocol was followed for the ELISA assays. As a negative control in all experiments, fresh culture medium containing serum was used, to compensate for endogenous levels of growth factors that may have been present in serum.

2.6 Subcutaneous Implantation and Analysis of ADSCs in Fibrin

ADSCs were pre-labeled with DiI (Invitrogen) per the manufacturer's recommendations for 1 hr at 37°C. Following labeling, the ADSCs were loaded into the fibrinogen component of the fibrin sealant kit as described above. The fibrin gels containing the ADSCs were subcutaneously injected into the ventral side of the mouse and left in place for seven days. Following the seven-day incubation, the mouse received a 100 μL tail vein injection of high molecular weight FITC-dextrans ($MW > 1 \times 10^6$; Sigma) immediately prior to sacrifice. The fibrin gels were explanted and prepared for immunostaining as described above. All mice

used for experiments were C57/B6 (female) between 8–12 weeks of age. Mice received 3 fibrin subcutaneous implants each (n=9 technical replicates).

2.7 Full Thickness Rodent Wounds and ADSC Fibrin Implantation

Full thickness back wounds were created using a 6 mm biopsy punch. Mice were anesthetized with a mixture of ketamine/xylazine, the backs were shaved, and the skin folded over followed by application of the 6 mm biopsy punch such that two 6 mm symmetrical full thickness wounds were created. All mice used for wounding experiments were C57/B6 (female) between 8–12 weeks of age (n=5). Immediately following the creation of the full thickness wounds, approximately $0.30 – 0.50 \times 10^6$ ADSCs were delivered in 250–300 μl of fibrin gel directly onto the wound. The conditions for these experiments included ADSCs delivered in either Composition 1 or Composition 2 fibrin formulation, a no treatment control, and a fibrin gel of Composition 1 only, with no cells, as a further control. After application of the gels, a Tegaderm bandage was placed over the wound. The mice were allowed to heal for 5 days prior to sacrifice and analysis of the wound closure stage was done. Standard histological analysis performed included H&E and Masson's Trichrome.

Mice also received DiI pre-labeled cells—described above—delivered in the topical fibrin treatment in order to track the fate of the cells.

2.8 Scanning Electron Microscopy

Gel samples were prepared for scanning electron microscopy (SEM) by fixation and dehydration. Briefly, gels were washed with PBS and fixed with SEM fixative (2.5% glutaraldehyde/2.0% paraformaldehyde mixture in 0.2 M sodium cacodylate) for 30 minutes at 37°C, followed by 2 hour incubation at 4°C. The samples were post-fix processed in 1% osmium tetroxide in the same buffer for one hour. The samples were dehydrated following a standard ethanol series. After critical point drying, samples were imaged on an XL-30 ESEM.

Statistical Analyses

All experiments were repeated at least three times and each condition was analyzed in triplicate. The data were expressed as mean SEM (standard error of measurement). Unpaired, two-tailed Student's t-tests were performed to evaluate whether the two groups were significantly different from each other. $p \leq 0.05$ was considered statistically significant.

3 Results

3.1 ADSC characterization

Human adipose liposuction materials were digested with collagenase type 1, centrifuged and the stromal cell fraction was expanded in 10% FBS/DMEM on tissue culture plastic. Cells were assayed by FACS for MSC marker expression between passages 2 and 5. ADSCs were positive for canonical MSC markers including CD73, CD90 and CD105 while being negative for CD45 and Mac-1 (Supplementary Figure 1). We also assessed whether there was endothelial cell contamination within our cultures by performing FACS analysis with

markers used to detect endothelial cells CD31 (PECAM-1) and VE-cadherin (CD144). All of our ADSC cultures between passages 2–5 were largely negative for the endothelial cell markers assessed (<1% abundance of cells with endothelial markers, Supplementary Figure 1 and Figure 1).

3.2 Immunohistochemical, FACS and qRT-PCR analysis of ADSC-embedded fibrin gels

The stiffness of the fibrin gel was changed by adjusting the stoichiometric ratios of fibrinogen and thrombin. Previous work has shown that matrix stiffness modulates MSC differentiation [28] and that increasing the concentration of either fibrinogen or thrombin in the formulation of fibrin gels results in gels that are stiffer [29]. The ADSCs were embedded into two fibrin formulations that varied in the concentrations of both fibrinogen and thrombin: a stiff fibrin gel we termed Composition 1 (223 KIU/ml thrombin; 36.6 mg/ml fibrinogen) and a softer fibrin gel termed Composition 2 (145 KIU/ml thrombin; 23.6 mg/ml fibrinogen). The ADSC fibrin mixtures were dispensed into chamber slides and cultured in 10% FBS/DMEM for analysis (Figure 1). By day 7, in culture there appeared branched, tube-like structures exclusively in the ADSCs that were embedded in fibrin Composition 1 (Figure 1A). The ADSCs that were mixed with Composition 2 fibrin did not form branching, tube-like structures, and the cells mostly remained spherical in appearance (Figure 1D).

We performed immunohistochemical analysis, FACS and qRT-PCR to assess whether the ADSC expressed endothelial cell or pericyte markers (Figure 1). Immunostaining for the pericyte marker, NG2, revealed large, numerous branching structures present within Composition 1 fibrin gels (Figure 1A). Although there was detectable expression of NG2 within the ADSCs embedded in Composition 2 fibrin gels, there was no evidence of branching structures (Figure 1D). We infected the ADSCs with eGFP lentivirus to make visualization of the tube structures easier within the gels. With these eGFP-transfected ADSCs, we were able to discern VE-cadherin+ structures that contained clear lumens (Figure 1C).

For quantification of the ADSCs that expressed endothelial makers within the fibrin gel, we assayed for the expression of VE-cadherin by FACS analysis after 2 weeks of culture (Figure 1B, E). Approximately 49% of the ADSCs cultured for 2 weeks in Composition 1 fibrin gels expressed VE-cadherin, whereas only 5% of cells cultured in Composition 2 fibrin gels expressed this marker. ADSCs cultured on tissue culture plastic were VE-cadherin negative (Figure 1F).

qRT-PCR data showed that cells cultured in Composition 1 fibrin gels (C1) had 65 to 105 fold increased expression of VE-cadherin on days 7 and 14, respectively, relative to ADSCs on tissue culture plates. There was also a detectable increase in the VE-cadherin fold expression in ADSCs that had been cultured in Composition 2 fibrin gels (C2); however, the level of expression was less than that present in cells cultured in Composition 1 fibrin gels (Figure 1G; $p<0.05$). qRT-PCR for CD31 expression also revealed an increase expression of CD31 relative to ADSCs cultured on tissue culture plastic. There was also a statistically significant difference in CD31 expression between cells cultured in Composition 1 and 2, wherein cells in Composition 1 had greater expression of CD31 at day 7 and 14 (Figure 1H;

$p<0.05$). These findings indicate that, while both fibrin gels seemed to increase the expression of endothelial-associated markers by MSC, the stiffer formulation appeared to do so more strongly. Increased endothelial marker expression was associated with increased formation of tubular-like structures visible in the gel at Day 14.

3.3 Rheological characterization of fibrin Composition 1 and Composition 2

Rheological characterization was performed on the fibrin gels made of Composition 1 and 2 (Figure 2A). Composition 1 gels were higher concentration and stiffer, with a storage modulus of 3,000 Pa, and the Composition 2 gels were softer and have a storage modulus of 1,650 Pa. By scanning electron microscopy, Composition 1 gels had a more compact microfibrillar organization (Figure 2B) as compared to Composition 2 gels (Figure 2D). Additionally, the microfibrillar structures in the Composition 1 gel had a rougher appearance, or higher rugosity. Microfibrillar structural differences within fibrin gels have previously been shown to have an affect on cell phenotype [30], and may likely play a role in marker expression of ADSC in these gels.

Collectively, these data support the concept that ADSCs are capable of forming tubes in stiffer (higher concentration) fibrin gels, and that the cells in those tubes upregulate markers associated with endothelium, in addition to some pericyte markers.

3.4 ELISA analysis of bFGF secretion by Composition 1 and Composition 2 fibrin gels

ELISA analyses were performed for bFGF, PDGF-BB, VEGF and KGF. While there were no significant differences in the amount of PDGF-BB, VEGF or KGF secreted by the cells in either condition (data not shown), there was consistently greater expression of bFGF by cells cultured in Composition 1 fibrin gels, on days 7 and 21, as compared to Composition 2 (Figure 3A). These data were particularly interesting given that endothelial-to-mesenchymal transitions are partly dependent on bFGF [31]. ELISAs were repeated three times, with samples run as duplicates.

We followed these experiments by attempting to “rescue” the branching phenotype in ADSCs grown in Composition 2 gels by spiking the culture medium with bFGF (4 ng/ml). Data from these experiments show that we are able to induce branching structures from ADSCs following 7 days of culture in Composition 2 fibrin gels (Figure 3B–D). These data indicate that cytokine signaling pathways may play a role in allowing the ADSCs to develop into branching, tubular structures within fibrin gels.

3.5 Subcutaneous in vivo transplantation of Composition 1 and Composition 2 fibrin gels in mice

We next assayed whether the ADSC blood vessel-like structures were capable of forming perfusable tubes *in vivo*. For these experiments, ADSCs were labeled with DiI, and mixed with fibrin gel components and injected subcutaneously into a mouse model. The fibrin plug containing ADSCs embedded in either Composition 1 or Composition 2 gels were injected and left subcutaneously for 7 days. At the 7-day mark, and prior to sacrificing the animal, the mice were perfused with high molecular weight FITC-dextrans via tail vein injection, in an effort to highlight vascular beds. The extracted fibrin plugs were processed for

immunostaining for endothelial cell markers. Consistent with the *in vitro* work, the DiI labeled ADSCs in the Composition 1 fibrin gels formed large, dense branching structures that were positive for CD31. Importantly, these ADSC tubular structures contained regions of FITC-dextran perfusate (Figure 4). The ADSCs in fibrin Composition 2 did not form any blood vessel structures (Figure 4I) and generally appeared not to survive well since few DiI+ cells were detected after 7 days culture. These data show that the ADSCs in Composition 1 fibrin gels contribute to perfused blood vessels when placed subcutaneously. Additionally, these data support the notion that fibrin composition is critical in coaxing the ADSCs to participate in the formation of perfusable blood vessels.

3.6 Topical application of Composition 1 and Composition 2 fibrin gels in rodent full-thickness wound model

We next assessed whether ADSCs delivered topically would allow for quicker wound healing when compared to no treatment or with a fibrin-only material devoid of cells. To this end, 6-mm full thickness wounds were created on the backs of C57/B6 mice (total animals: 7; total wounds analyzed: 14) followed by immediate application of topical ADSCs within fibrin gels of Composition 1. The fibrin gels were held in place with a Tegaderm bandage and the wound was assessed at day 5. As controls for these experiments, certain mice received fibrin only (made of Composition 1), and others that received no treatment were also included in our analyses. Gross measurements at day 5 did not reveal large differences in wound closure sizes across all groups (data not shown). However, ADSCs delivered topically in fibrin Composition 1 resulted in healing wounds that histologically showed more granulation tissue and blue-staining collagen when compared to fibrin only treatment or no treatment (Figure 5). The amount of granulation tissue, as opposed to subcutaneous adipose tissue, is oftentimes used as a metric to assess the healing stages of the wound. Collagen deposition was assessed through Masson's trichrome, showing that ADSCs within fibrin gels of Composition 1 leads to a dramatic increase on the amount of collagen present at day 5 as compared to the fibrin-only and the no treatment conditions (Figure 5).

3.7 Immunohistochemical analysis of topically delivered ADSCs in mouse model

Following the initial full thickness skin-wounding event, ADSCs were pre-labeled with DiI and delivered topically in Composition 1 fibrin gels (Figure 6). When explanted at day 5, the ADSCs appeared to remain within the fibrin and did not cross into the granulation tissue of the healing wound (Figure 6A). These data support the concept that the ADSCs have a beneficial effect through the secretion of cytokines that recruit host cells that aid in the wound healing process.

We also stained for CD31+ cells within, and closely juxtaposted to, the granulation tissue (Figure 6B, D), as well as the presence of smooth muscle actin (SMA) positive cells (Figure 6C, E). Immunofluorescence staining revealed that there was an increase in the amount of CD31+ cells at the sites of wound closure in the Composition 1 fibrin gels containing ADSCs (Figure 6B), whereas there is a paucity of CD31+ cells in the wounds treated with fibrin gels that did not contain the ADSCs (Figure 6D). Similarly, the amount of SMA

positive cells was greater in the Composition 1 fibrin gels (Figure 6C) that contained the MSCs when compared with animals that had not received any treatment (Figure 6E).

4. Discussion

We have developed a fibrin formulation that results in the formation of perfusable blood vessel structures derived from human adipose tissue mesenchymal stromal cells (ADSCs). We have demonstrated a potential role for fibrin gel concentration in the formation of tubular and perfusable structures derived from human MSCs. Gel concentration can affect the density, stiffness and substrate composition. Additionally, we have shown that full thickness skin wounds in rodents treated with ADSCs delivered in a topical fibrin sealant leads to acceleration of wound closure when compared to animals receiving topical administration of fibrin sealant without cells. ADSCs are an ideal source for cell delivery in cases of chronic, non-healing wounds and in cases of delayed wound healing. One of the large benefits of ADSCs is that they can be easily isolated from patient samples by punch biopsy and expanded for several passages allowing for an autologous source of cells for topical application [32].

In vitro characterization of the ADSCs showed that the formation of blood vessel-like, tubular structures was dependent on the fibrin formulation in which these cells were grown. Specifically, it was apparent that the stiffer fibrin formulation (Composition 1) allowed for highly branched structures to form, whereas the softer fibrin formulation (Composition 2) did not allow for the formation of branching structures. Interestingly, there is a connection between fibrin formulation and the stiffness of the resultant gel [29]. Previous work has shown that substrate characteristics, including substrate stiffness, may play a role in the differentiation of progenitor cells [33] and MSCs [26]. Whereas Zhang et al. [27] reported a modulus of up to 173 Pa for MSC differentiation into an EC-like phenotype, our study aligns with results from Wingate [26] in demonstrating that a stiffer gel formulation on the order of 2 + 1 kPa is necessary for promoting an EC-like phenotype. This may make sense given that the compressive modulus of the *in vivo* endothelial basement membrane is between 2–3 kPa [34]. Collectively these prior studies have indicated that matrix concentration and consequent stiffness may have an effect on cell phenotype.

Additionally, other groups have used various MSC sources in different gels systems to demonstrate direct formation of functional blood vessels. A recent manuscript has suggested that PEGylated fibrin gels can support the formation of *de novo* blood vessels following topical application to wounds [35]. The authors find that the adipose MSCs allow for the enhanced formation of blood vessels following topical delivery of these constructs onto wounds, some of which they suggest may be derived from the adipose MSCs delivered in the PEGylated fibrin gels. However, our data clearly show that ADSCs in fibrin-only gels have the ability to form blood vessel-like structures *in vitro* that have markers of endothelial cells, and *in vivo*. Subcutaneous implants show that the human-derived adipose MSCs reside in vessels that anastomose with the rodent host vasculature system, and express localized markers of mature endothelial cells (Figure 6). Interestingly, the ability of the cells to become functional blood vessels as determined by active perfusion through the vessels was

directly dependent on the fibrin formulation; the ADSCs embedded in the stiffer fibrin formulation (C1) had this ability, whereas the softer formulation (C2) did not.

The ability to form tubular structures in fibrin gels appears to be closely linked to the presence of bFGF within the culture medium. bFGF is a pro-angiogenic cytokine that mediates mitogeneis of endothelial cells *in vivo* and induces an angiogenic response. Previous studies have solidified a link between the maintenance of endothelial cell phenotype, and the presence of bFGF and the inhibition of TGFβ [28]. Through the addition of exogenous bFGF within the culture medium of the softer fibrin gels, we were able to partially rescue the branching phenotype to levels similar to those seen with the stiffer fibrin formulation. These data support the notion that bFGF not only plays a role in the endothelial-to-mesenchymal transition that has been previously reported [28], but also play a role in the opposite direction in promoting a mesenchymal-to-endothelial phenotype in ADSCs embedded in fibrin gels.

We also investigated whether ADSCs delivered in the stiff fibrin formulation would accelerate full thickness wound healing in rodent models. Many studies have shown a benefit in the use of mesenchymal stromal cells in accelerating wound closure [3, 5, 7, 35, 36]. Our data using ADSCs delivered topically in stiff fibrin gels onto full thickness wounds show a clear benefit of ADSC cell delivery versus fibrin only or no treatment of the wound. Previous studies have shown that mesenchymal stromal cells may accelerate wound closure through the secretion of cytokines, including bFGF [3, 9]. In addition to its role in angiogenesis, bFGF stimulates the proliferation of fibroblasts in a dose-dependent manner [37]. Our data supports a paracrine role, with the secretion of bFGF, rather than a direct contribution of MSCs to the healing wound, in contrast to what other groups have found [38]. This discrepancy may largely be due to the MSCs in the previous experiment being directly injected into the periphery of the wound rather than topical application of MSCs in fibrin gel as we have performed. When subcutaneously administered to rodents, we do not find any evidence of ADSCs directly giving rise to endothelial cells within the healing wound itself; rather, these cells mostly remain in the periphery of the wound within the fibrin construct. While restriction of the cells to the fibrin compartment may partly be due to the fibrin formulation itself, we did not find any differences between cell-delivery in soft versus the stiff fibrin formulation with regards to ultimate MSC location (data not shown).

Non-healing or slowly healing wounds are a prevalent complication resulting from various pathologies, including diabetes and irradiation treatment following skin cancer resection [1]. These chronic or non-healing wounds have been shown to respond positively in human clinical trials when bone-marrow MSCs were applied topically via fibrin sealant [3]. Our research supports these prior observations and further demonstrates that the ADSCs, while not directly incorporating into the wound, have a beneficial effect in the acceleration of the wound healing process. Future studies will focus on the ability to use MSCs delivered in appropriate vehicles that facilitates their potential to directly or indirectly contribute to angiogenesis in wound healing applications, as well as in tissue engineered organs and tissues.

5.0 Conclusions

Our study demonstrates that ADSCs can be induced to form tubular structures in stiff fibrin gels. ADSCs cultured in this system express markers of endothelial cells as shown by RT-PCR, immunostaining, and *in vivo* subcutaneous functional assays. The ability of ADSCs to form the tubular structures is directly related to the concentration of the gels in which these cells are cultured. Additionally, we show that topical delivery of ADSCs within stiff fibrin gels onto full thickness wounds results in the acceleration of wound healing when compared to no treatment, or to stiff fibrin devoid of cells. Together, these data support that ADSCs are capable of both forming tubular structures and accelerating wound healing, which occurs through an indirect, paracrine-mediated fashion. These observations can potentially have beneficial effects for future clinical wound healing trials.

Supplementary Material

Refer to Web version on PubMed Central for supplementary material.

Acknowledgments

J.J.M is supported by NIH T32 GM086287; LEN is also supported by NIH R01 HL098220.

References

1. Haubner F, Ohmann E, Pohl F, Strutz J, Gassner HG. Wound healing after radiation therapy: Review of the literature. Radiation Oncology. 2012; 7(1)
2. Singer AJ, Clark RAF. Cutaneous Wound Healing. New England Journal of Medicine. 1999; 341(10):738–46. [PubMed: 10471461]
3. Falanga V, Iwamoto S, Chartier M, Yufit T, Butmarc J, Kouttab N, et al. Autologous bone marrow-derived cultured mesenchymal stem cells delivered in a fibrin spray accelerate healing in murine and human cutaneous wounds. Tissue Eng. 2007; 13(6):1299–312. [PubMed: 17518741]
4. Shaw TJ, Martin P. Wound repair at a glance. Journal of Cell Science. 2009; 122(18):3209–13. [PubMed: 19726630]
5. Fathke C, Wilson L, Hutter J, Kapoor V, Smith A, Hocking A, et al. Contribution of Bone Marrow–Derived Cells to Skin: Collagen Deposition and Wound Repair. Stem Cells. 2004; 22(5):812–22. [PubMed: 15342945]
6. Sorrell JM, Caplan AI. Topical delivery of mesenchymal stem cells and their function in wounds. Stem Cell Research & Therapy. 2010; 1(4)
7. Sorrell JM, Baber MA, Caplan AI. Influence of adult mesenchymal stem cells on in vitro vascular formation. Tissue Eng Part A. 2009; 15(7):1751–61. [PubMed: 19196139]
8. Ravari H, Hamidi-Almadari D, Salimifar M, Bonakdaran S, Parizadeh MR, Koliakos G. Treatment of non-healing wounds with autologous bone marrow cells, platelets, fibrin glue and collagen matrix. Cytotherapy. 2011; 13(6):705–11. [PubMed: 21284564]
9. Wu Y, Chen L, Scott PG, Tredget EE. Mesenchymal stem cells enhance wound healing through differentiation and angiogenesis. Stem Cells. 2007; 25(10):2648–59. [PubMed: 17615264]
10. Ra JC, Shin IS, Kim SH, Kang SK, Kang BC, Lee HY, et al. Safety of intravenous infusion of human adipose tissue-derived mesenchymal stem cells in animals and humans. Stem Cells and Development. 2011; 20(8):1297–308. [PubMed: 21303266]
11. Wakabayashi K, Nagai A, Sheikh AM, Shiota Y, Narantuya D, Watanabe T, et al. Transplantation of human mesenchymal stem cells promotes functional improvement and increased expression of neurotrophic factors in a rat focal cerebral ischemia model. J Neurosci Res. 2010; 88(5):1017–25. [PubMed: 19885863]

12. Vailhé B, Vittet D, Feige JJ. In vitro models of vasculogenesis and angiogenesis. Lab Invest. 2001; 81(4):439–52. [PubMed: 11304563]

13. Warrier S, Haridas N, Bhonde R. Inherent propensity of amnion-derived mesenchymal stem cells towards endothelial lineage: vascularization from an avascular tissue. Placenta. 2012; 33(10):850–8. [PubMed: 22840296]

14. Pierantozzi E, Gava B, Manini I, Roviello F, Marotta G, Chiavarelli M, et al. Pluripotency regulators in human mesenchymal stem cells: expression of NANOG but not of OCT-4 and SOX-2. Stem Cells and Development. 2011; 20(5):915–23. [PubMed: 20879854]

15. Zhen-Zhou C, Xiao-Dan J, Gui-Tao L, Jiang-Hua S, Ling-Hui L, Mou-Xuan D, et al. Functional and ultrastructural analysis of endothelial-like cells derived from bone marrow stromal cells. Cytotherapy. 2008; 10(6):611–24. [PubMed: 18836916]

16. Alviano F, Fossati V, Marchionni C, Arpinati M, Bonsi L, Franchina M, et al. Term amniotic membrane is a high throughput source for multipotent mesenchymal stem cells with the ability to differentiate into endothelial cells in vitro. BMC Dev Biol. 2007; 7(1):1–14. [PubMed: 17199897]

17. Benavides OM, Petsche JJ, Moise KJ, Johnson A, Jacot JG. Evaluation of Endothelial Cells Differentiated from Amniotic Fluid-Derived Stem Cells. Tissue Engineering Part A. 2012; 18(11–12):1123–31. [PubMed: 22250756]

18. Gang EJ, Jeong JA, Han S, Yan Q, Jeon CJ, Kim H. In vitro endothelial potential of human UC blood-derived mesenchymal stem cells. Cytotherapy. 2006; 8(3):215–27. [PubMed: 16793731]

19. Chen M-Y, Lie P-C, Li Z-L, Wei X. Endothelial differentiation of Wharton's jelly–derived mesenchymal stem cells in comparison with bone marrow–derived mesenchymal stem cells. Experimental Hematology. 2009; 37(5):629–40. [PubMed: 19375653]

20. Bai K, Huang Y, Jia X, Fan Y, Wang W. Endothelium oriented differentiation of bone marrow mesenchymal stem cells under chemical and mechanical stimulations. Journal of Biomechanics. 2010; 43(6):1176–81. [PubMed: 20022602]

21. Zhang P, Baxter J, Vinod K, Tulenko TN, Di Muzio PJ. Endothelial Differentiation of Amniotic Fluid–Derived Stem Cells: Synergism of Biochemical and Shear Force Stimuli. Stem Cells and Development. 2009; 18(9):1299–308. [PubMed: 19508152]

22. Lin H, Shabbir A, Molnar M, Yang J, Marion S, Canty JM, et al. Adenoviral expression of vascular endothelial growth factor splice variants differentially regulate bone marrow-derived mesenchymal stem cells. J Cell Physiol. 2008; 216(2):458–68. [PubMed: 18288639]

23. Duffy GP, D'Arcy S, Ahsan T, Nerem RM, O'Brien T, Barry F. Mesenchymal Stem Cells Overexpressing Ephrin-B2 Rapidly Adopt an Early Endothelial Phenotype with Simultaneous Reduction of Osteogenic Potential. Tissue Engineering Part A. 2010; 16(9):2755–68. [PubMed: 20491587]

24. Xu J, Liu X, Chen J, Zacharek A, Cui X, Savant-Bhonsale S, et al. Simvastatin enhances bone marrow stromal cell differentiation into endothelial cells via notch signaling pathway. American Journal of Physiology - Cell Physiology. 2009; 296(3):C535–C43. [PubMed: 19109527]

25. Colley H, McArthur SL, Stolzing A, Scutt A. Culture on fibrin matrices maintains the colony-forming capacity and osteoblastic differentiation of mesenchymal stem cells. Biomed Mater. 2012; 7(4)

26. Wingate K, Bonani W, Tan Y, Bryant SJ, Tan W. Compressive elasticity of three-dimensional nanofiber matrix directs mesenchymal stem cell differentiation to vascular cells with endothelial or smooth muscle cell markers. Acta Biomaterialia. 2012; 8(4):1440–9. [PubMed: 22266031]

27. Zhang G, Drinnan CT, Geuss LR, Suggs LJ. Vascular differentiation of bone marrow stem cells is directed by a tunable three-dimensional matrix. Acta Biomaterialia. 2010; 6(9):3395–403. [PubMed: 20302976]

28. Park JS, Chu JS, Tsou AD, Diop R, Tang Z, Wang A, et al. The effect of matrix stiffness on the differentiation of mesenchymal stem cells in response to TGF-β. Biomaterials. 2011; 32(16):3921–30. [PubMed: 21397942]

29. Duong H, Wu B, Tawil B. Modulation of 3D fibrin matrix stiffness by intrinsic fibrinogen-thrombin compositions and by extrinsic cellular activity. Tissue Eng Part A. 2009; 15(7):1865–76. [PubMed: 19309239]

30. Hall H, Baechi T, Hubbell JA. Molecular properties of fibrin-based matrices for promotion of angiogenesis in vitro. Microvasc Res. 2001; 62(3):315–26. [PubMed: 11678634]

31. Chen P-Y, Qin L, Barnes C, Charisse K, Yi T, Zhang X, et al. FGF regulates TGF-β signaling and endothelial-to-mesenchymal transition via control of let-7 miRNA expression. Cell Rep. 2012; 2(6):1684–96. [PubMed: 23200853]

32. Francis MP, Sachs PC, Elmore LW, Holt SE. Isolating adipose-derived mesenchymal stem cells from lipoaspirate blood and saline fraction. Organogenesis. 2010; 6(1):11–4. [PubMed: 20592860]

33. Trappmann B, Gautrot JE, Connelly JT, Strange DGT, Li Y, Oyen ML, et al. Extracellular-matrix tethering regulates stem-cell fate. Nat Mater. 2012; 11(7):642–9. [PubMed: 22635042]

34. Peloquin J, Huynh J, Williams RM, Reinhart-King CA. Indentation measurements of the subendothelial matrix in bovine carotid arteries. Journal of Biomechanics. 2011; 44(5):815–21. [PubMed: 21288524]

35. Zamora DO, Natesan S, Becerra S, Wrice N, Chung E, Suggs LJ, et al. Enhanced wound vascularization using a dsASCs seeded FPEG scaffold. Angiogenesis. 2013; 16(4):745–57. [PubMed: 23709171]

36. Harris DT, Hilgaertner J, Simonson C, Ablin RJ, Badowski M. Cell-based therapy for epithelial wounds. Cytotherapy. 2012; 14(7):802–10. [PubMed: 22458955]

37. Makino T, Jinnin M, Muchemwa FC, Fukushima S, Kogushi-Nishi H, Moriya C, et al. Basic fibroblast growth factor stimulates the proliferation of human dermal fibroblasts via the ERK1/2 and JNK pathways. Br J Dermatol. 2010; 162(4):717–23. [PubMed: 19995368]

38. McFarlin K, Gao X, Liu YB, Dulchavsky DS, Kwon D, Arbab AS, et al. Bone marrow-derived mesenchymal stromal cells accelerate wound healing in the rat. Wound Repair Regen. 2006; 14(4):471–8. [PubMed: 16939576]

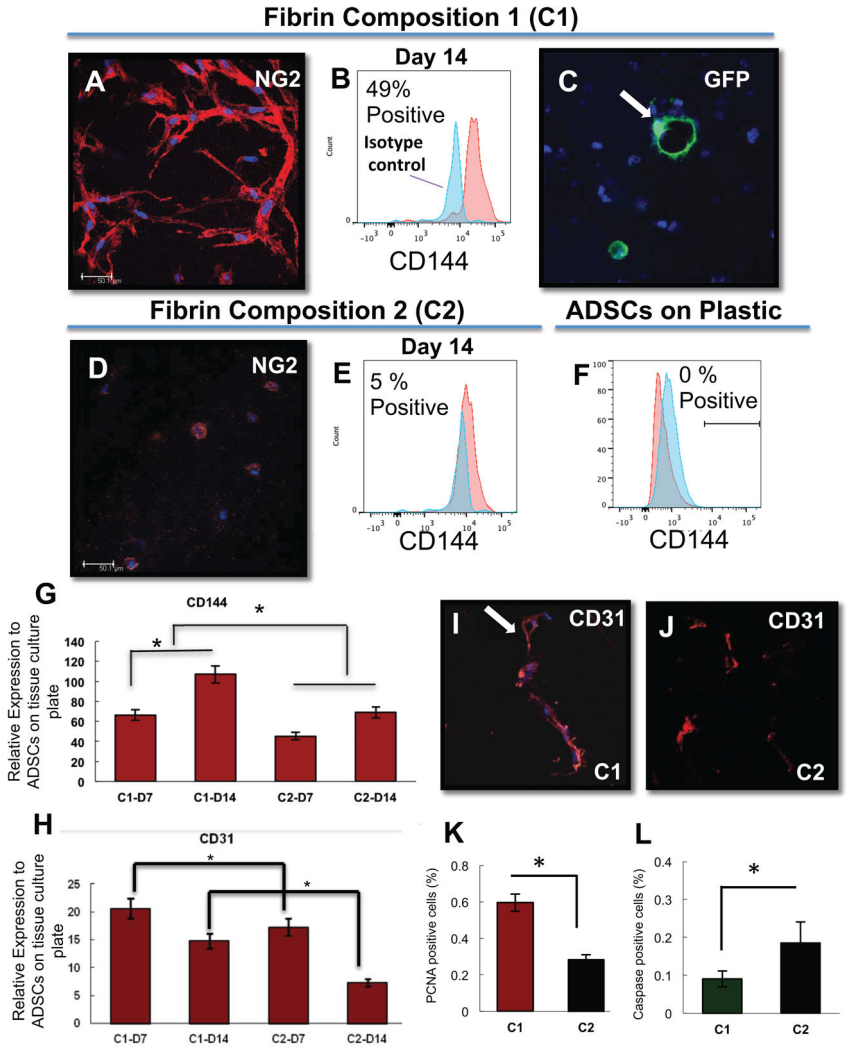

Figure 1.

ADSCs form tube structures within the stiffer fibrin gels (Composition 1) and express endothelial cell markers as assessed by FACS, immunohistochemistry, and qRT-PCR. (A,D) At day 7 of culture, ADSC-derived, NG2 +, cellular tube structures (red) are present in fibrin gel cultures at composed of stiff fibrin formula (A) and not in the less stiff formula (D). (B, E) The stiff fibrin conditions also allow for expression of CD144 in up to 49% of the population over isotype control by FACS (B), whereas only 5% of the population in the softer formula is CD144+ (E). GFP-ADSCs also form hollow tube/luminal structures in Composition 1 fibrin gels at Day 7 (C). A comparison with cells cultured on plastic tissue culture flasks (F) reveals that there is no CD144 population present in this condition. (G,H) PCR data indicates increased EC marker presence in stiff compared to soft fibrin formulation. C1-D7, C1-D14 = fibrin Composition 1 Day 7 and 14, respectively; C2-D7, C1-D14 = fibrin Composition 2 day 7 and 14 respectively. (I, J) Immunostaining for CD31 in fibrin conditions C1 and C2, with an arrow pointing to the lumen. Quantification of PCNA+ cells (K) and caspase + cells (L) in fibrin conditions C1 and C2. Scale bar = 50 μm, nuclei are counterstained with DAPI (blue). N=3 technical replicates for each condition

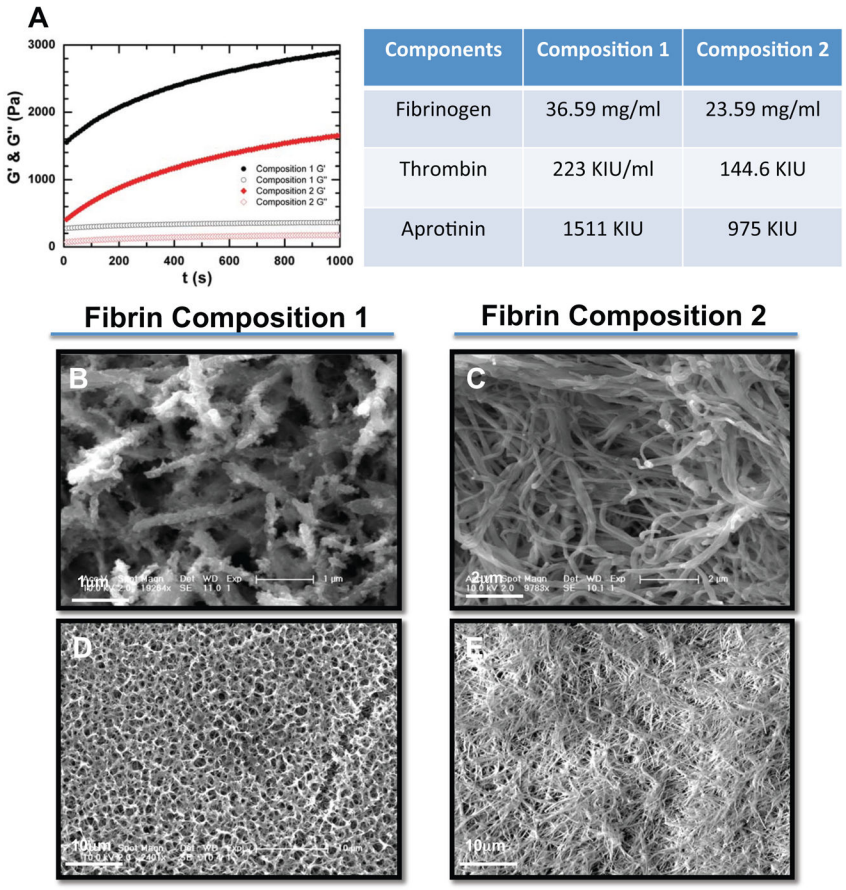

Figure 2.

Rheological and SEM analysis of fibrin gel compositions reveal stiffness and structural differences. (A) Elasticity (G′ full circles) and loss modulus (G″ open circles) of Composition 1 fibrin gels plotted in black, and Composition 2 fibrin gels plotted in red as a function of time. The storage modulus G was 3000 Pa for the Composition 1 gels, and 1650 Pa for Composition 2 gels. The table shows the stoichmetric ratios of fibrinogen, thrombin and aprotinin in Composition 1 and 2 (B–E) SEM micrographs show Composition 1 fibrin gels have fibrils with a higher rugosity, scale bar = 1mm (B) when compared with the fibrils of Composition 1, scale bar = 2mm (C). Additionally, the Composition 1 fibrin gels (D) have a greater porosity than the Composition 2 gels (E), scale bars = 10μm

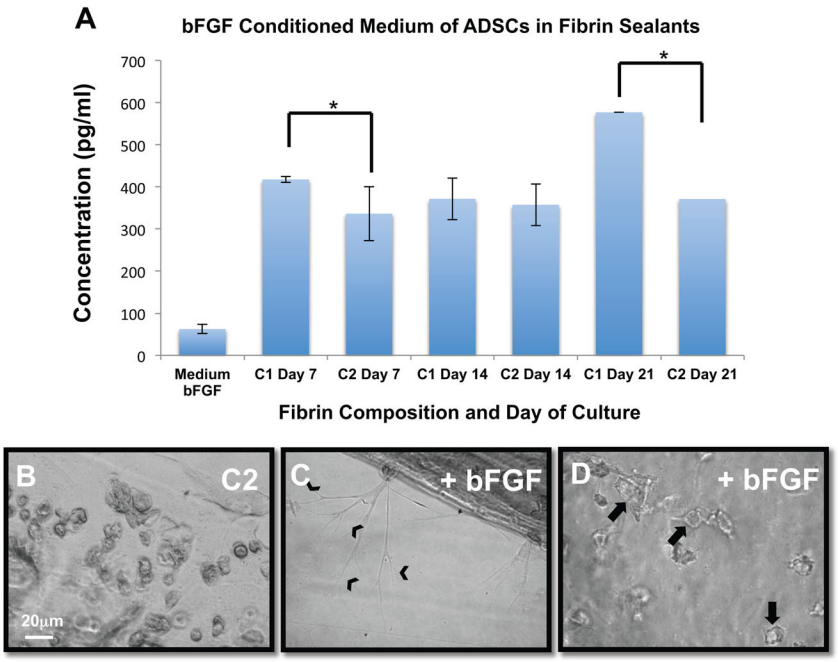

Figure 3.

The presence of bFGF in the culture medium is associated with the increased ability of ADSCs to form tubular structures. (A) bFGF ELISA indicates that there is higher bFGF concentration in the conditioned medium in which ADSCs were grown in Composition 1 gels when compared with Composition 2 gels, at days 7 and 21. N=3 (samples run as duplicates). *$p<0.05$, bars represent SEM. (B–D) ADSCs grown in Composition 2 fibrin gels in which the medium was spiked with bFGF (C–D), contained cells that formed branching structures (chevrons in C), and also contained cells that formed luminal structures (arrows in D) when compared to the non-bFGF spiked condition (B). Scale bar = 20 μm

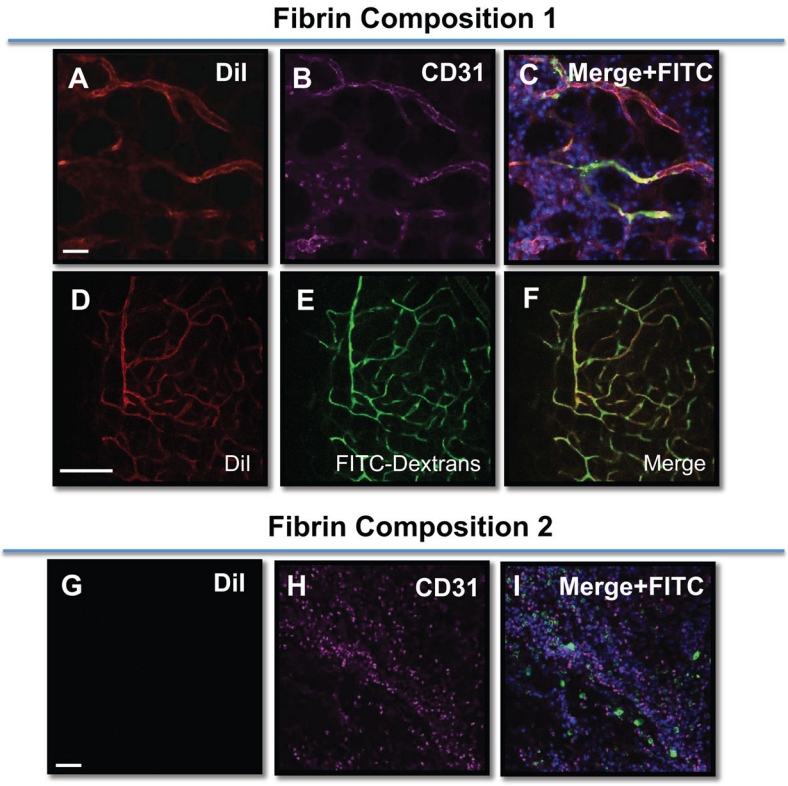

Figure 4.

ADSCs anastomose with the host vasculature and express endothelial markers. Composition 1 fibrin gels (A–F) or Composition 2 fibrin gels (G-1) containing DiI-labeled ADSCs (red) were subcutaneously implanted in mice and left in place for 7 days. Prior to the sacrifice of the animal, the animal received FITC-dextrans (green) via a tail vein injection. The ADSCs contained within Composition 1 fibrin gels formed clear, multi-branching structures (A–F) that were ADSC derived (DiI+, A, D), and contained FITC-dextrans within the lumens of these structures (C, E). Additionally, these structures were positive for the endothelial cell marker, CD31 (magenta) (B). (G–I) In contrast, very few ADSCs remained in the Composition 2 fibrin gels that were implanted and there was no evidence of FITC-dextran perfused, DiI+ vessels. Scale bar = 50 μm for all images. Nuclei are counterstained with DAPI (blue) in (C,I)

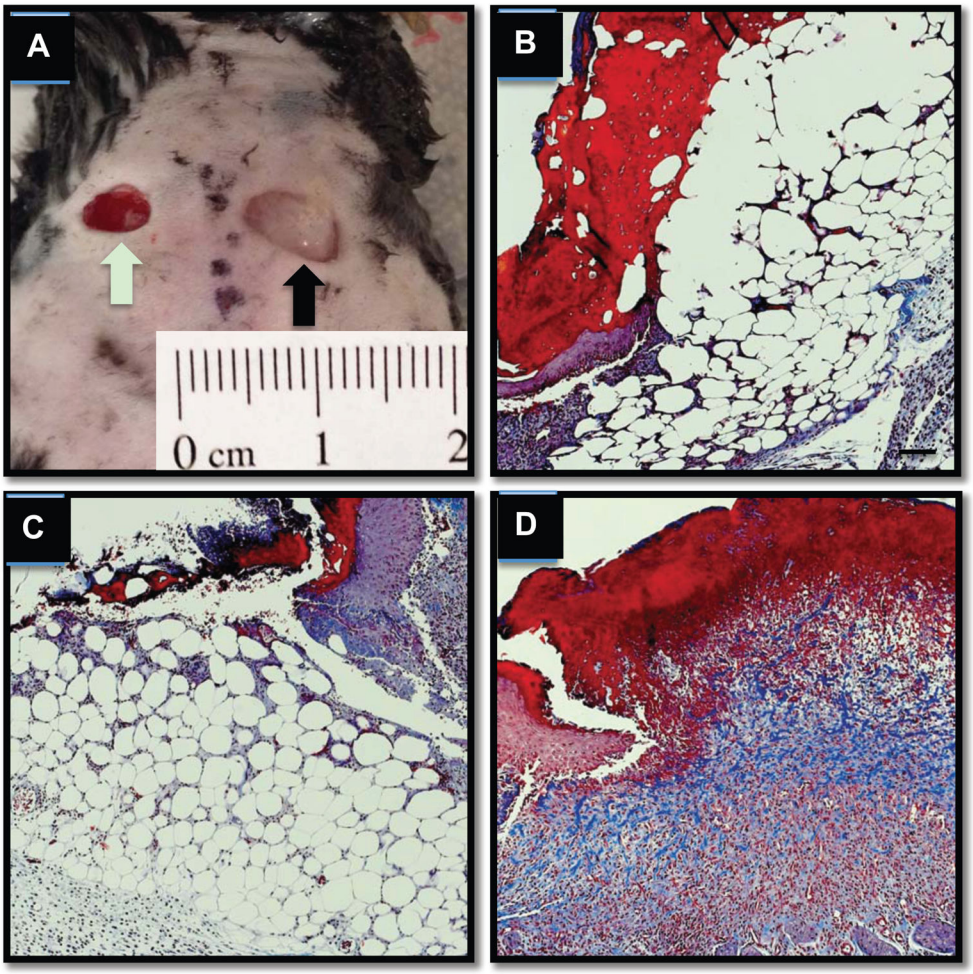

Figure 5.

Collagen deposition (shown via Masson's trichrome stain in blue above) by ADSCs delivered in a stiff fibrin composition (A) Symmetrical 6 mm full-thickness wounds were created on the backs of C57/B6 mice followed by no treatment (B and green arrow in A), administration of stiff formulation fibrin only containing no cells (C, and black arrow in A), or stiff fibrin formulation with 0.5×10^6 ADSCs (D). Significant granulation tissue and collagen deposition at day 5 of wound healing.

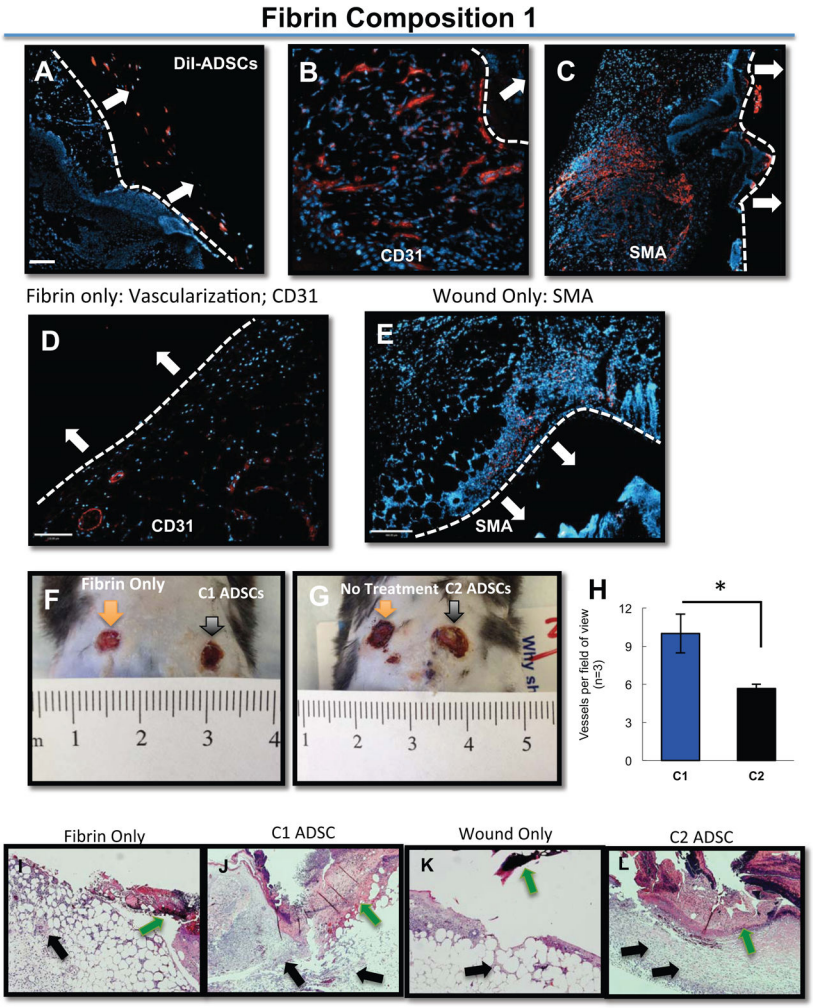

Figure 6.

ADSCs remain in the periphery of the wound and within the fibrin gels (A) ADSCs were pre-labeled with DiI and embedded within Composition 1 gels and placed topically over full-thickness mouse wounds; ADSCs remain in the periphery of the wound, and remain encapsulated within the fibrin itself. (B–C) Non-labeled ADSCs were placed topically over full thickness wounds in Composition 1 fibrin gels; CD31 (B) expression and SMA expression (C) is evident when compared to either fibrin only (D) or with the wound only, no treatment condition (E), which are negative for both markers. All secondary antibodies are shown in red. The white bar and white arrows in each of the panels identifies the apex of the healing wound. The white arrows point to the location of the fibrin sealant. (F, G). There are a significantly higher number of vessels per field of view in C1 gels as compared to C2 (H). C1 or C2 gels, respectively, delivered onto full-thickness rodent wounds. In the fibrin-only condition (I), there is not a significant gross histological distinction from the wound-only (K), whereas with C1 gels (J), there is more granulation tissue and cellularity compared to C2 gels (L). Nuclei are counterstained with DAPI (blue). Scale bar = 50 μm